Drug Delivery and Translational Research (2019) 9:97–105
https://doi.org/10.1007/s13346-018-0577-6

ORIGINAL ARTICLE

Development and biological evaluation of a new nanotheranostic for tuberculosis

Edward Helal-Neto[1] · Suyene Rocha Pinto[1] · Filipe Leal Portilho[1] · Marcellus Dias da Costa[2] · Jonathas Xavier Pereira[3] · Fiammetta Nigro[4] · Eduardo Ricci-Junior[4] · Andre Luis Peixoto Candéa[5] · Maria das Graças Muller de Oliveira Henriques[5] · Ralph Santos-Oliveira[1,6]

Published online: 3 September 2018

Abstract

In this study, we developed, characterized, and tested in vivo polymeric nanoparticle of ethambutol labeled with 99mTc as nanoradiopharmaceutical for early diagnosis of tuberculosis by single-photon emission computed tomography, also as a therapeutic choice. Nanoparticles were developed by double emulsification. All characterization tests were performed, as scanning electron microscopy and dynamic light scattering. The labeling process with 99mTc was performed using the direct labeling process. In vitro and in vivo assays were performed with animals and cells. The results showed that a spherical ethambutol nanoparticle with a size range of 280–300 nm was obtained. The stability test showed that the nanoparticles were well labeled with 99mTc (> 99.1%) and keep labeled over 24 h. The biodistribution assay showed that almost 18% of the nanoparticles were uptake by the lung in infected mice (male C57Bl/6) with *Mycobacterium bovis* BCG (4×10^5 CFU/cavity), corroborating its use as a nanodrug for tuberculosis imaging. The results for the cell assay corroborate its therapeutical effect. We developed and efficiently tested a new nanodrug that can be used for both imaging and therapy of tuberculosis, acting as a novel nanotheranostic.

Keywords Radiopharmaceuticals · Nanotechnology · Smart device · Infection

Abbreviations

TB	Tuberculosis
BK	Koch's bacillus
99mTc	Technetium 99 metastable
SPECT	Single-photon emission computed tomography
mCi	Milli Curie
MBq	Mega Becquerel
RPMI	Roswell Park Memorial Institute medium
PVA	Polyvinyl alcohol
PCL	Polycaprolactone
DLS	Dynamic light scattering
SEM	Scanning electron microscopy
NIH	National Institutes of Health
BCG	Bacillus Calmette–Guérin
CFU	Colony-forming units
PBS	Phosphate-buffered saline
PFA	Paraformaldehyde
EMB	Ethambutol
PDI	Polydispersity index
EPR	Enhanced permeability and retention

✉ Ralph Santos-Oliveira
roliveira@ien.gov.br

[1] Brazilian Nuclear Energy Commission, Nuclear Engineering Institute, Rio de Janeiro, Brazil

[2] Fiocruz Foundation, National Institute of Infectology, Rio de Janeiro, Brazil

[3] Institute of Biomedical Science, Laboratory of Proliferation and Cell Differentiation, Federal University of Rio de Janeiro, Rio de Janeiro, Brazil

[4] College of Pharmacy, Galenical Development Laboratory, Federal University of Rio de Janeiro, Rio de Janeiro, Brazil

[5] Laboratory of Applied Pharmacology, Farmanguinhos, Oswaldo Cruz Foundation, Rio de Janeiro, Brazil

[6] Laboratory of Radiopharmacy and Nanoradiopharmaceuticals, Zona Oeste State University, Rio de Janeiro, Brazil

Introduction

Tuberculosis (TB) is a global public health problem due to the high prevalence in many countries and is closely linked to the socioeconomic conditions. Approximately 33% of the world's

population has latent tuberculosis infection, which means that at some point those 33% of the world's population may develop TB. In number, TB represents 10.4 million cases with 1.4 million deaths in 2016 [1, 2]. Factors that hinder their effective control in the world are associated with problems involving prevention, diagnosis, treatment, quality of health services, and peculiarities of users with tuberculosis [3–5].

The disease, which is infectious and contagious, is caused by the bacterium Mycobacterium tuberculosis, also called Koch's bacillus (BK). Transmission occurs through droplets containing bacilli expelled by a patient with pulmonary tuberculosis when coughing, sneezing, or talking. When these droplets containing bacilli are inhaled by healthy people reaching the alveoli, the infection can be established [6–8].

Tuberculosis is a serious disease, but curable in practically 100% of the cases. The main drugs used in standard treatments are the following: isoniazid—H, rifampicin—R, and pyrazinamide—ethambutol and ZE [9]. Rapid and precise diagnosis of infected patients is determinant for tuberculosis control strategies. Besides, the increase number of multidrug resistance [10] is increasing the demand of new drugs with a higher technological complex, especially the use of nanoparticles [11, 12]. The development of a drug carrier that can efficiently deliver antituberculosis drugs encapsulated is a helpful theranostic strategy [13]. It was already demonstrated that 99Tc-EMB has high potential to qualify as a specific tuberculosis imaging radiopharmaceutical and is safe for human use [14]. Also, in a recent study, graphene oxide with iron oxide magnetite nanoparticles that was loaded with ethambutol showed potent antitubercular activity while remaining nontoxic to the eukaryotic cells tested [12].

In this direction, this work has developed nanoradiopharmaceuticals based on ethambutol polymeric nanoparticles labeled with 99mTc for theranostic strategy of TB.

Materials and methods

Development of ethambutol nanoparticle

To the nanoparticle preparation, an ethambutol tablet (400 mg of ethambutol hydrochloride, oral administration) was triturated, and then, an amount containing 5 mg of ethambutol was weighted (which represents 10% of the polymer mass to be added to the nanoparticle) and solubilized in 0.1 wt% PVA aqueous solution.

Ethambutol nanoparticles were prepared by double-emulsion solvent evaporation method where 200 μL of ethambutol-PVA aqueous solution was dripped into 2 mL of dichloromethane, where 50 mg of PCL (with a molar mass of 42,000 g/mol) was previously solubilized and then sonicated (UP100H, Hielscher) for 1 min at 55 W to produce a water-in-oil emulsion. This emulsion was emulsified again with 4 mL of PVA 1 wt% solution by ultrasound processing for 2 min (55 W) to produce a W/O/W emulsion. Then, dichloromethane was evaporated under reduced pressure during 1 h at 25 °C. PCL-NPs were recovered by centrifugation (20,000 rpm for 20 min) and washed twice with distilled water to remove the excess of PVA. At the end, only PCL-ethambutol nanoparticles were used.

Size determination by DLS

Nanoparticle size distribution, mean size, and polydispersity index (PDI) of the ethambutol nanoparticle were determined by dynamic light scattering (DLS) using the equipment Zetasizer Nano ZS (Malvern Instruments, UK). Measurements were performed in triplicate at 25 °C, and the laser incidence angle in relation to the sample was 173° using a 12-mm^2 quartz cuvette. The mean ± standard deviation (SD) was assessed.

Scanning electron microscopy

Nanoparticle morphology was examined by scanning electron microscopy (SEM) (TM 3000, Hitachi), with a tension varying from 10 to 20 kV. The sample, 10 μL of the nanoparticle solution was fixed on a carbon tape and dried under aseptic conditions.

Stability

In order to evaluate the stability of the nanoparticle, mimicking a human biological condition, the mircoparticle solution (100 μL) was incubated with human albumin solution (20%) Grifols®, and after 5, 10, 30, 45, 60, 90, 120, and 240 min, the nanoparticles were recovered by centrifugation and analyzed by SEM microscopy, using the same methodology described in "Scanning electron microscopy" section.

Labeling process with 99mTc

The labeling process was done using 150 μg of each ethambutol nanoparticle incubated with stannous chloride ($SnCl_2$) solutions (80 μL/mL) (Sigma-Aldrich) for 20 min at room temperature. Then, this solution was incubated with 100 μCi (approximately 300 μL) of technetium-99m for another 10 min in order to label their structures.

In vivo analysis

Animals

Male C57Bl/6 (18–30 g) were obtained from Oswaldo Cruz Foundation breeding unit and lodged in a room with controlled temperature (23 ± 2 °C) and lighting, with free access

to lab chow and tap water. All experiments were conducted in accordance with the NIH guide for the care and use of laboratory animals and approved by the Oswaldo Cruz Foundation experimental animal ethics committee.

Materials

Lyophilized *Mycobacterium bovis*-BCG (Moreau strain) was obtained from Fundação Ataulpho de Paiva (Rio de Janeiro, Brazil) and the colony-forming unit (CFU) numbers provided by National Institute of Quality Control in Health (INCQS-FIOCRUZ, Rio de Janeiro, Brazil).

Mycobacterial infection

Mycobacterial infection (tuberculosis) was induced as described by Henriques et al. [15]. Briefly, an adapted needle (13 × 5 gauge) was inserted carefully 2 mm through the parietal pleura into the right side of the thoracic cavity of mice to enable injection of 100 mL of *M. bovis* BCG (4×10^5 CFU/cavity). Control animals received an equal volume of sterile saline. Mice were sacrificed by CO_2 inhalation 24 h, 15 days, or 30 days after the inoculation, and their thoracic cavities were opened and flushed with 1 mL of heparinized phosphate-buffered saline (PBS; 40 IU/mL).

Biodistribution

Mice were maintained under controlled temperature (23 °C ± 2) with water and food ad libitum. No anesthetic was used. The labeled samples (3.7 MBq/0.2 mL) were administered by intraocular (retro-orbital) injection. After 2 h of drug administration, mice were sacrificed by asphyxiation (CO_2 chamber) and then dissected, and their lungs were removed, weighed, and the radioactivity uptake counted in a gamma counter (PerkinElmer). Results were expressed as percentage of injected dose per gram of tissue. The Institutional Review Board and the Animal Ethics Committee approved the study protocol (CEUA-IPEN 182/2017).

Histological analysis of tuberculosis

After tuberculosis induction, the right lungs were collected 1, 15, and 30 days post-induction; cleaved; and

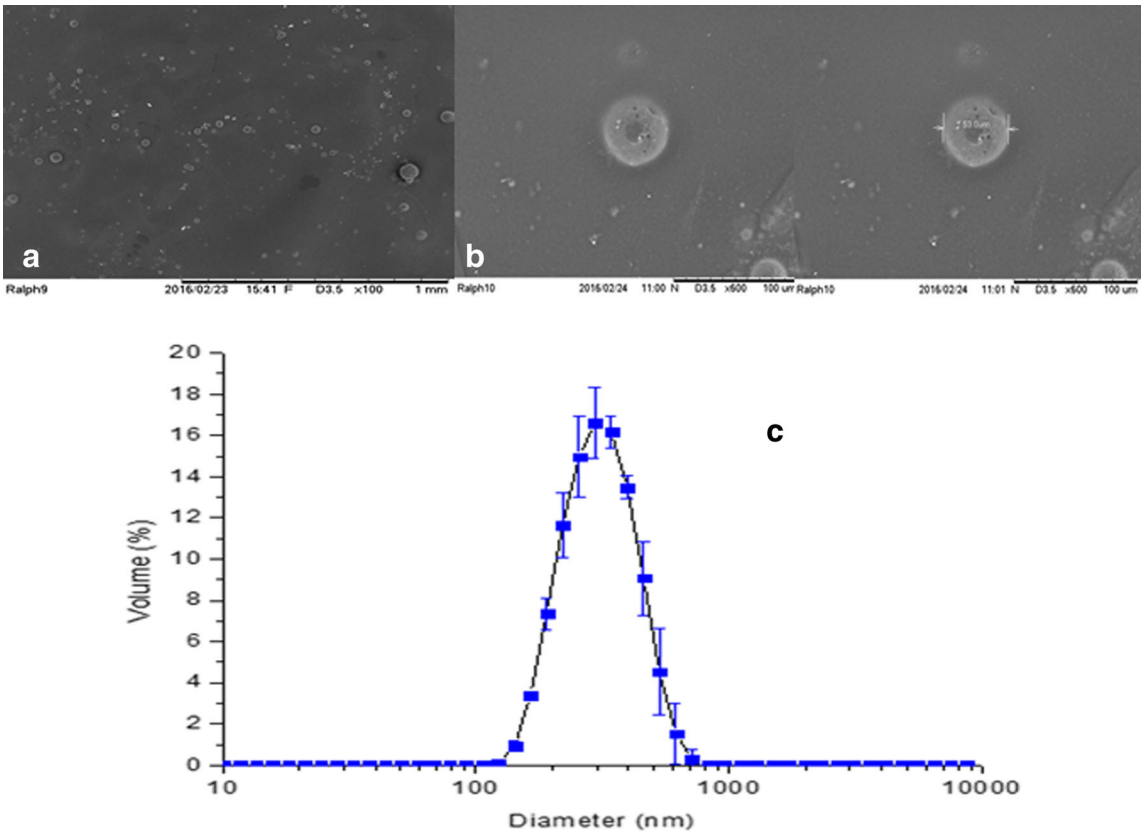

Fig. 1 **a** Immediate SEM imaging showing nanoparticle with a range size of 280–320 nm with reduced formation of aggregates. **b** SEM imaging 10 days post-nanoparticle formulation confirming the possibility of aggregation with aggregates size range from 320 to 500 nm. **c** Immediate DLS mean size and size distribution of the ethambutol nanoparticles corroborating the SEM imaging (**a**) showing a medium size of 270 nm

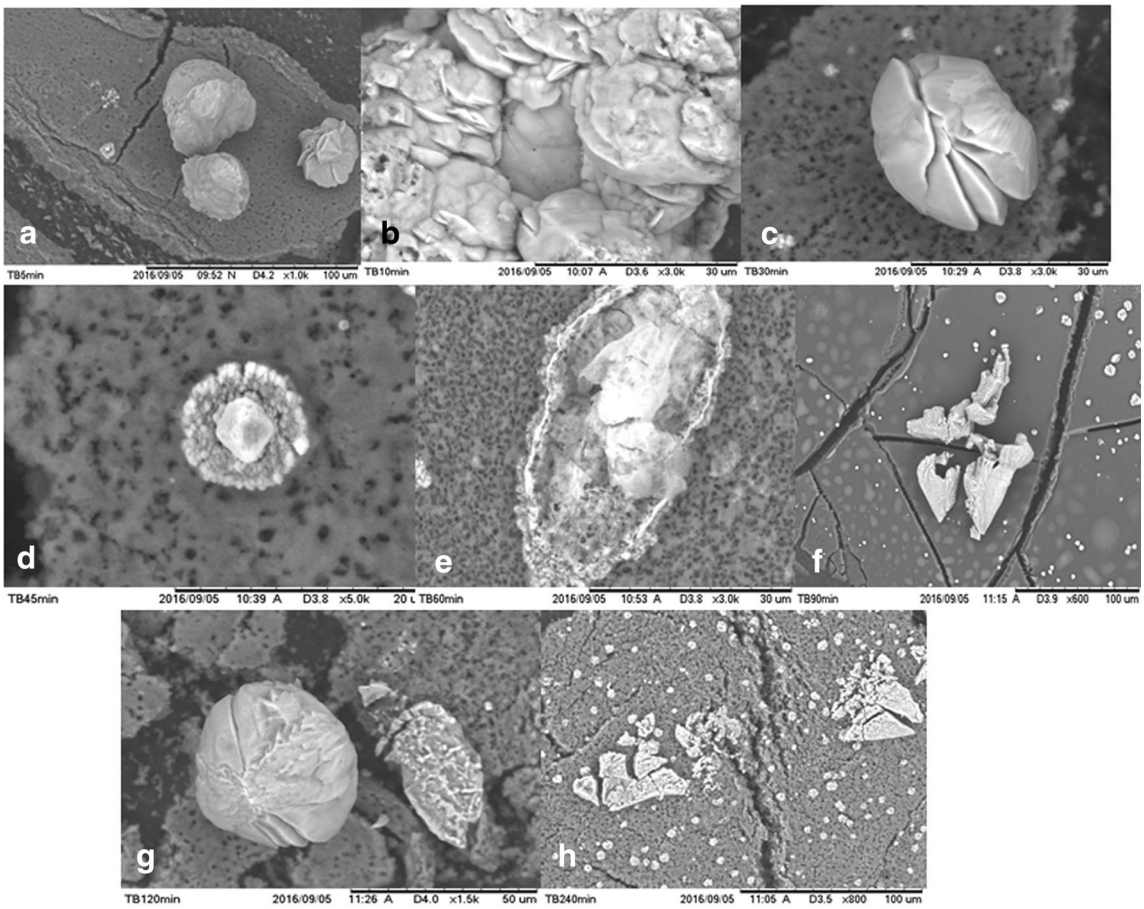

Fig. 2 SEM images showing the stability of the nanosystem during time after incubation with albumin, in order to mimetize the blood protein composition. **a** Five-minute time of incubation of ethambutol nanoparticles. It is possible to observe the very complete nanoparticle. **b** Ten-minute time of incubation of ethambutol nanoparticles showing the aggregation of the nanoparticle and the interaction (surrounding) with the bacteria. **c** Thirty-minute time of incubation of ethambutol nanoparticles, showing the integrity of the nanoparticle. **d** Forty-five-minute time of incubation of ethambutol nanoparticles, showing the degradation begging of nanosystem. **e** Sixty-minute time of incubation of ethambutol nanoparticles, demonstrating the high degradation rate. **f** Ninety-minute time of incubation of ethambutol nanoparticles, showing the breakup of the nanoparticle and consequent release of the ethambutol. **g** One-hundred-twenty-minute time of incubation of ethambutol nanoparticles, showing the release process and the sustained delivery of ethambutol. It is possible to observe a well-degraded nanoparticle next to a totally intact one. **h** Two-hundred-forty-minute time of incubation of ethambutol nanoparticles. Total degradation of the nanoparticle

fixed in 4% PFA. The paraffin-embedded tissues were sliced with a thickness of 4 μm and stained with H&E and Ziehl Neelsen staining. The Ziehl Neelsen staining was carried out following Weldu et al. [16].

The slides were flooded with filtered 1% carbol fuchsine and heated until steaming but not boiling for 5 min. After slides had been rinsed with tap water, 3% acid alcohol was used to decolorize smears for 3 min. Then, slides were rinsed and counterstained with 0.1% methylene blue for 1 min. Finally, the slides were washed, air-dried, and examined using an oil immersion objective. The composition of the reagents was as follows: 1% carbol fuchsine: basic fuchsine 10 g, molten phenol 50 mL, 95% ethanol 100 mL, and distilled water 850 mL; 3% acid alcohol: 96% ethanol 970 mL and hydrochloric acid 30 mL; and 0.1% methylene blue: methylene blue 1 g and distilled water 1000 mL. The staining color was quantified using ImageJ software.

Table 1 Percentage of labeled nanoparticles after ascending chromatograms of ^{99m}Tc compared with free pertechnetate ($Na^{99m}TcO_4^-$)

Time (h)	Labeling (%)
0	99.52 ± 1.2
1	99.45 ± 1.3
2	99.55 ± 1.0
4	99.21 ± 1.1

Culture and growth of *M. bovis* BCG-GFP in vitro

Aliquots of *M. bovis* BCG strain expressing GFP (BCG-GFP) were cultured at 37 °C in Middlebrook 7H9 medium supplemented with 10% oleic acid/albumin/dextrose/

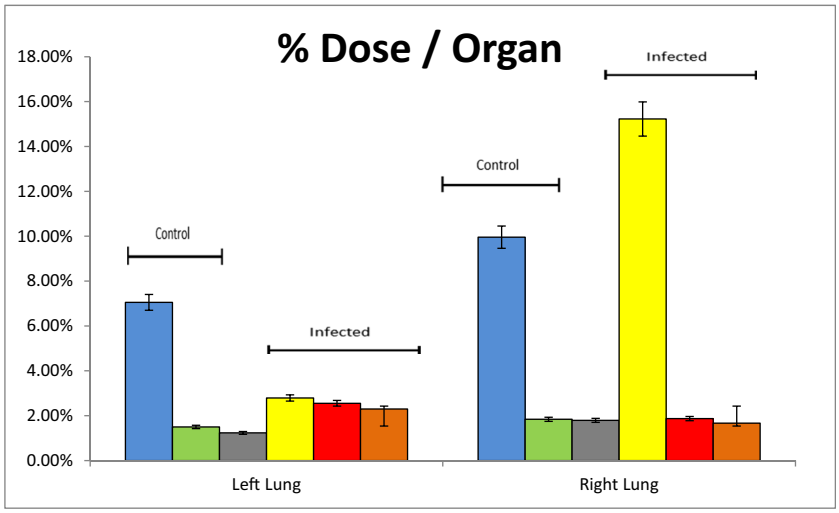

Legend: blue: healthy animals 24 hours. Green: healthy animals 15 days. Grey: healthy animals 30 days. Yellow: infected animals 24 hours. Red: infected animals 15 days. Orange: Infected animals 30 days.

Fig. 3 Biodistribution of the 99mTc-ethambutol nanoparticle into inducted animals compared with the controls (healthy animals). This figure corroborates the biodirection of the nanoparticles and its imaging effect due the high uptake by the lungs. In blue, we have healthy animals which have received nanoparticles 24 h post-infection. In green, we have healthy animals which have received nanoparticles 15 days post-infection. In gray, we have healthy animals which have received nanoparticles 30 days post-infection. In yellow, we have the nanoparticle evaluation in inducted mice 24 h post-infection. In red, we have the nanoparticle evaluation in inducted mice 15 days post-infection. In orange, we have the nanoparticle evaluation in inducted mice 30 days post-infection

catalase (OADC) and Tween-80 (0.05%) plus kanamycin (25 μg/mL). Bacterial growth quantification was performed by quantification of absorbance (O.D. 600 nm) and fluorescence (E_x 488 nm, E_m 520 nm) in the SpectraMax M5 multimodal reader (Molecular devices, USA).

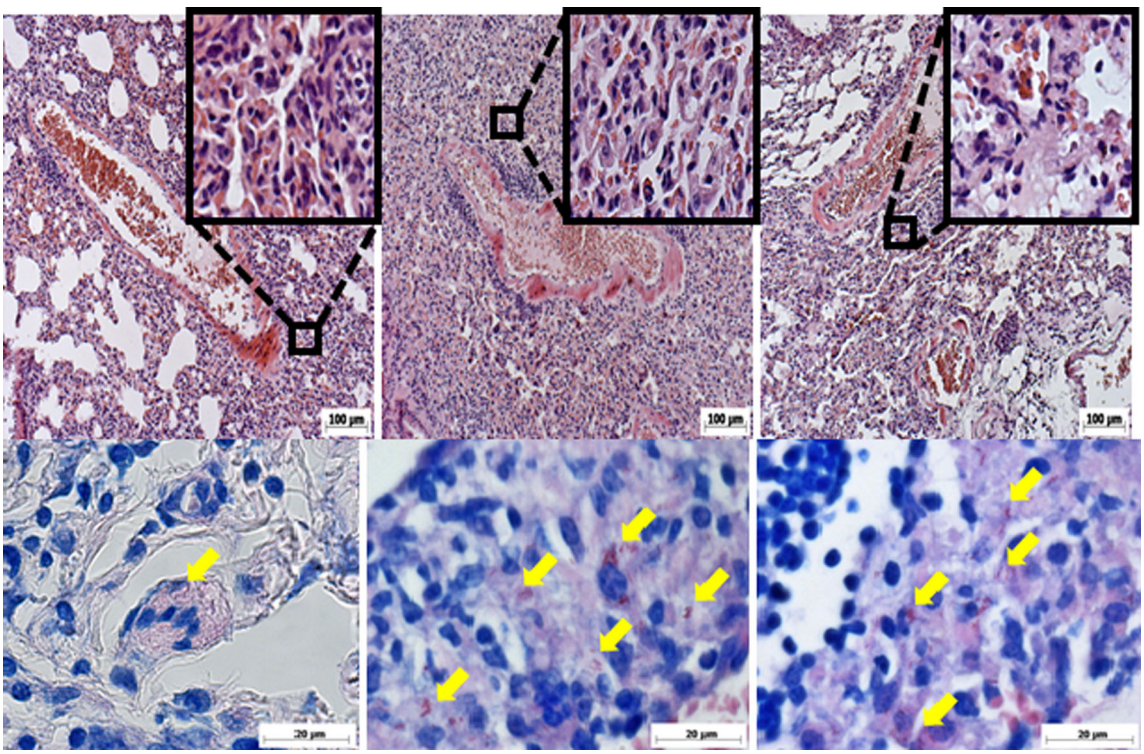

Fig. 4 Histopathological analysis of mice infected lungs. The yellow narrows are point out the presence of bacilli. The presence of the bacilli in all stages of infection corroborates the methodology

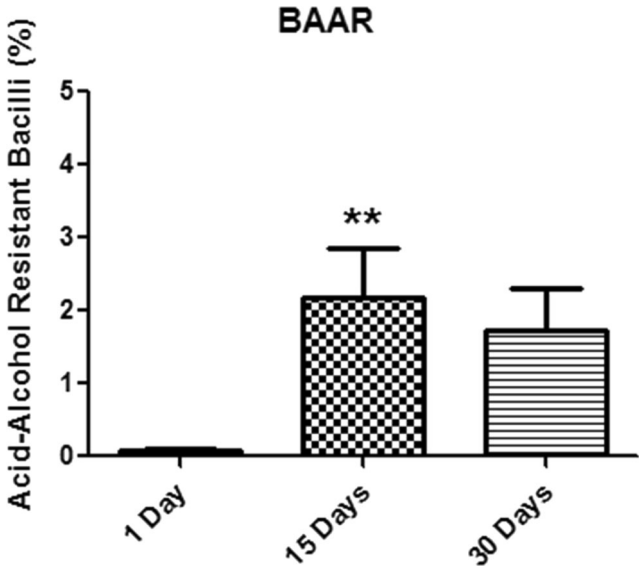

Fig. 5 Acid-fast bacilli (Ziehl Neelsen) reaction, demonstrating the presence of the bacilli in all lungs, corroborating the findings of the histopathological analysis

Activity assay of *M. bovis* BCG GFP growth in macrophages in vitro

Cells from murine J774 A1 macrophages lineage were cultured in RPMI-1640 supplemented with 10% fetal bovine serum (FBS) and 0.1% gentamycin. 1 × 105 cells were plated in 24-well plates on glass coverslips for 24 h at 37 °C with 5% CO_2. BCG-GFP strain was grown to the log growth phase (≈14 days) in supplemented Middlebrook 7H9 medium. Prior to infection, the bacteria were washed two times with buffer solution. The infection was performed in the multiplicity of infection (MOI) ratio 5:1 bacteria for macrophages in a volume of 500 μL/well. BCG-GFP were incubated with macrophages for 4 h. After, cells were incubated for 24 h with ethambutol (12 mg/kg) alone or with nanoparticles loaded or not with ethambutol. Cells were then fixed in 4% paraformaldehyde for 30 min at room temperature, labeled with DAPI (1:10,000), and mounted for capture in a fluorescence microscopy. The stained coverslips were examined under a NIKON ECLIPSE microscope equipped for epifluorescence. Analysis was performed by counting the percentage of infected macrophages by fluorescence microscopy (objective ×60; Nikon, Japan).

Statistical

The statistical analyses were performed using GraphPad Prism 6.0 software (GraphPad Software, Inc.). Results are shown as means ± standard deviation (S.D.). To determine statistically significant differences between groups, normal distribution was assumed and one-way analysis of variance (ANOVA) was used. $p < 0.05$ was considered as statistically significant.

Results and discussion

The results from SEM (Fig. 1) showed that nanoparticles size was about 280–300 nm. A late SEM image demonstrated that nanoparticles may aggregate, forming a nanoparticle with a size no bigger than 500 nm (Fig. 1) 10 days post-formation of the nanosystem.

Thus, considering the circumference volume (Cv) equation,

$$Cv = \pi r^3$$

where Cv is the circumference volume, Π is the constant pi, r is the radius of the circumference.

The molar mass of PCl is 66.4268 g/mol. As also the medium average size of the ethambutol nanoparticle of 290 nm, we have that the weight of one single ethambutol nanoparticle is about 3.6×10^{-15} g.

DLS size characterization

Figure 1 shows the mean size and size distribution of the ethambutol nanoparticles. According to the distribution profile, it is possible to infer that nanoparticles presented a monomodal size distribution, with a mean size of 270 nm, corroborating the findings of SEM. The narrow peak suggests a homogeneous system with sizes near to the mean. According to Paranjpe and Müller-Goymann [17], particles smaller than 500 nm were deposited in the alveolar region; sediment could be retained in the bronchiolar region for a longer time when compared to nanoparticles, which could improve efficacy.

Stability

In order to evaluate the stability of the nanoparticle with serum medium, a series of images were done in different times (5, 10, 30, 45, 60, 90, 120, and 240 min) with nanoparticle solution incubated with a human albumin solution (20%; Fig. 2).

Labeling with 99mTc

The nanoparticles loaded with ethambutol were successfully labeled with 99mTc. The average of labeling efficacy was over 99%.

Quality control

The stability of the labeling process from the ethambutol nanoparticles with the 99mTc was checked, and the values are expressed in Table 1.

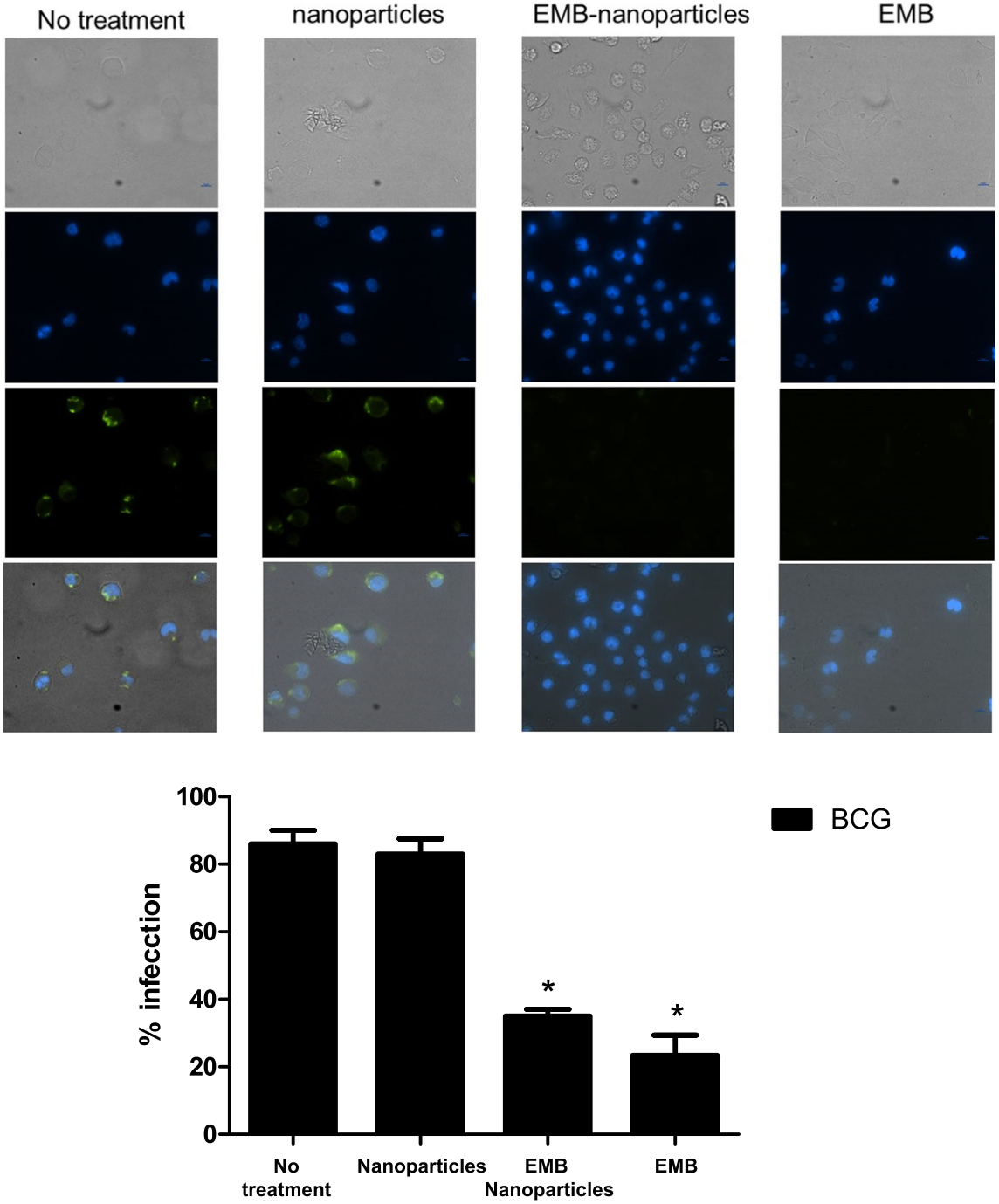

Fig. 6 Epifluorescence analysis of the ethambutol nanoparticle by fluorescence microscopy (objective ×60; Nikon, Japan), corroborating the nanoparticle interaction with the mycobacterial. The therapeutic effect of the nanoparticle performed by counting the percentage of infected macrophages is also shown

It is possible to observe that after 4 h, the 99mTc is still labeled with the ethambutol nanoparticle in a very high rate (> 99).

Biodistribution

Data from the biodistribution assay (Fig. 3) confirmed the biodirection and the enhanced permeability and retention (EPR) effect of the ethambutol (EMB)-labeled nanoparticle (EMB-99mTc). The most prominent effect was observed in 24-h-post-infected mice. This was expected due the fact that besides the infection, a local inflammation mimicking pleurisy would facilitate the accumulation of the nanoparticles in lung. Another point was the use of retro-orbital via, which follows the cava systemic via to reach the pulmonary veins and optimize the desired bioaccumulation. In 15-day-post-infected

mice, the most prominent results were found in the left lung, with a right lung showing no difference with the control group (non-infected mice). This may be explained by the fact that EMB is a bacteriostatic agent with a mechanism of action that inhibits mycobacterial cell wall synthesis. Thus, the primary role of EMB in the first-line four-drug antitubercular regimen (i.e., in combination with rifampin, isoniazid, and pyrazinamide) is to protect against rifampin resistance in the event of preexisting resistance to isoniazid [18]. Early biochemical studies showed that EMB was rapidly taken up by both replicating and non-replicating mycobacteria but active only against replicating bacilli, where it was found to impair glycerol metabolism as well as RNA synthesis [19–21]. In 30-day-infected mice, most of the infection entered in a log phase, with reduced glycerol metabolism as well as RNA synthesis. This might explain the low uptake of the EMB-99mTc nanoparticle. This is corroborated by the histopathological analysis (Figs. 4 and 5) due the observation of absence of nodule of Ghon, suggesting primary tuberculosis diagnosis associated with the involution of the disease 30 days post-infection.

An important finding is that even with low uptake, the amount of EMB-99mTc nanoparticle that has been uptake in the all the three infection models is sufficient to produce a single-photon computed tomography imaging, corroborating the use of EMB-99mTc nanoparticle as an imaging agent for TB, specially designed to be used for patients who have difficult or are unable to spit.

Histological analysis of tuberculosis

The histological analysis results showed segments of lungs demonstrating intense inflammatory reaction characterized by vascular congestion, thickening of alveolar septa, edema, and intense inflammatory infiltrate, formed basically of mononuclear cells. The inflammatory reaction was intense in the periods of 24 h and 15 days post-infection and with minor morphological changes in the period of 30 days post-infection. Some areas of hemorrhage were observed in all groups, as shown in Fig. 4. Results from the acid-fast bacilli (Ziehl Neelsen) reaction showed positivity in all groups and presence of bacilli in the cytoplasm of macrophages in perifollicular lymphoid regions (Fig. 5).

M. bovis BCG GFP growth in macrophages in vitro

Nanomedicine is a field in biomedical science where nanomaterials are designed and applied for theranostic applications. Since in this study we worked with a EMB-99mTc nanoparticle loaded with the therapeutic dose used for the treatment of the TB, we wonder about the theranostic effects of these nanoparticles.

Figure 6 demonstrates that EMB nanoparticle decreased the number of macrophage infected by mycobacterial and the amount of mycobacterial inside each infected macrophage when compared to group control. However, when macrophages were infected by mycobacterial and treated with nanoparticles alone, no differences were observed when compared to control group.

Viable bacilli are phagocytosed in the air spaces primarily by resident alveolar macrophages and dendritic cells. Following lung exposure, Mtb-infected phagocytes can migrate from the alveolar space into the lung interstitium and disseminate to other organs. Macrophages are the major host cell for the growth and survival of mycobacterial. The bacilli may grow unimpeded within host macrophages, resulting in primary progressive disease [22–24].

Noteworthy, EMB nanoparticles reduced mycobacterial infection with the same efficacy observed in macrophage infected and, then, treated with EMB alone.

Conclusion

Together with biodistribution data, the results observed at in vitro assays indicate that the nanoparticles used in this study present a theranostic effect. Thus, the ethambutol nanoparticle labeled with 99mTc can be used for TB imaging and therapy, and its use may be tested in human in order to corroborate its theranostic effect and in the future, belongs to a very specialized class of drugs to treat a very old disease.

Funding The authors would like to thank FAPERJ and CNPq for the financial support of this research.

Compliance with ethical standards

Conflicts of interest The authors declare that they have no conflicts of interest.

References

1. Corvino DFL, Kosmin AR. Tuberculosis, screening: StatPearls Publishing; 2017.
2. Bothamley G. The tuberculosis network European trials group (TBNET): new directions in the management of tuberculosis. Breathe. 2017;13(3):65–71.
3. Lin S, Melendez-Torres GJ. Critical interpretive synthesis of barriers and facilitators to TB treatment in immigrant populations. Tropical Med Int Health. 2017;22(10):1206–22.
4. Iacobino A, Piccaro G, Giannoni F, Mustazzolu A, Fattorini L. Fighting tuberculosis by drugs targeting nonreplicating Mycobacterium tuberculosis bacilli. Int J Mycobacteriol. 2017;6(3):213–21.
5. Xu Y, Wu J, Liao S, Sun Z. Treating tuberculosis with high doses of anti-TB drugs: mechanisms and outcomes. Ann Clin Microbiol Antimicrob. 2017;16(1):67.
6. Lim TK, Siow WT. Pneumonia in the tropics. Respirology. 2018;23(1):28–35.

7. Adigun R, Bhimji SS. Tuberculosis. Treasure Island: StatPearls Publishing; 2017.
8. Roya-Pabon CL, Perez-Velez CM. Tuberculosis exposure, infection and disease in children: a systematic diagnostic approach. Pneumonia (Nathan). 2016;24:8–23.
9. Zhang Y, Yew WW. Mechanisms of drug resistance in Mycobacterium tuberculosis. Int J Tuberc Lung Dis. 2009;13(11): 1320–30.
10. Ho J, Byrne AL, Linh NN, Jaramillo E, Fox GJ. Decentralized care for multidrug-resistant tuberculosis: a systematic review and meta-analysis. Bull World Health Organ. 2017;95(8):584–93.
11. Aderibigbe BA. Metal-based nanoparticles for the treatment of infectious diseases. Molecules. 2017;18:22–7.
12. Saifullah B, Maitra A, Chrzastek A, Naeemullah B, Fakurazi S, Bhakta S, et al. Nano-formulation of Ethambutol with multifunctional Graphene oxide and magnetic nanoparticles retains its antitubercular activity with prospects of improving chemotherapeutic efficacy. Molecules. 2017;12:22(10).
13. Pandey R, Khuller GK. Oral nanoparticle-based antituberculosis drug delivery to the brain in an experimental model. J Antimicrob Chemother. 2006;57:1146–52.
14. Singh N, Bhatnagar A. Clinical evaluation of efficacy of 99Tc-Ethambutol in tubercular lesion imaging. Tuberc Res Treat. 2010; 9 pages;2010:1–9.
15. Henriques MG, Weg VB, Martins MA, Silva PM, Fernandes PD, Cordeiro RS, et al. Differential inhibition by two hetrazepine PAF antagonists of acute inflammation in the mouse. Br J Pharmacol. 1990;99:164–8.
16. Weldu Y, Asrat D, Woldeamanuel Y, Hailesilasie A. Comparative evaluation of a two-reagent cold stain method with Ziehl-Nelseen method for pulmonary tuberculosis diagnosis. BMC Res Notes. 2013;6(323):13.
17. Paranjpe M, Müller-Goymann CC. Nanoparticle-mediated pulmonary drug delivery: a review. Int J Mol Sci. 2014;15(4):5852–73.
18. Bass JB, Farer LS, Hopewell PC, O'Brien R, Jacobs RF, Ruben F, et al. Treatment of tuberculosis and tuberculosis infection in adults and children. American Thoracic Society and the Centers for Disease Control and Prevention. Am J Respir Crit Care Med. 1994;149(5):1359–74.
19. Forbes M, Kuck NA, Peets EA. Mode of action of ethambutol. J Bacteriol. 1962;84:1099–103.
20. Kuck NA, Peets EA, Forbes M. Mode of action of ethambutol on Mycobacterium tuberculosis, strain H37R V. Am Rev Respir Dis. 1963;87:905–6.
21. Kilburn JO, Takayama K, Armstrong EL, Greenberg J. Effects of ethambutol on phospholipid metabolism in Mycobacterium smegmatis. Antimicrob Agents Chemother. 1981;19(2):346–8.
22. Hume DA, Ross IL, Himes SR, Sasmono RT, Wells CA, Ravasi T. The mononuclear phagocyte system revisited. J Leukoc Biol. 2002;72(4):621–7.
23. Guirado E, Schlesinger LS, Kaplan G. Macrophages in tuberculosis: friends or foe. Semin Immunopathol. 2013;35(5):563–83.
24. Frieden TR, Sterling TR, Munsiff SS, Watt CJ, Dye C. Tuberc Lancet. 2003;362(9387):887–99.